pubs.acs.org/acschemicalbiology

Articles

NMR-Based Metabolomics Approach to Explore Brain Metabolic Changes Induced by Prenatal Exposure to Autism-Inducing Chemicals

Ana Cristina Abreu, Miguel Morales Navas, Cristian Perez Fernández, Fernando Sánchez-Santed,* and Ignacio Fernández*

Cite This: *ACS Chem. Biol.* 2021, 16, 753–765

Read Online

ACCESS | Metrics & More | Article Recommendations | Supporting Information

ABSTRACT: NMR offers the unique potential to holistically screen hundreds of metabolites and has already proved to be a powerful technique able to provide a global picture of a wide range of metabolic processes underlying complex and multifactorial diseases, such as neurodegenerative and neurodevelopmental diseases. The aim of this study was to apply an NMR-based metabolomics approach to explore brain metabolic changes in both male and female rats induced by prenatal exposure to two chemicals associated with autism disorders—the organophosphorus pesticide chlorpyrifos (CPF) and the antiepileptic drug valproic acid (VPA)—at different postnatal ages. Depending on the age and on the brain region (hippocampus and cerebellum), several metabolites were shown to be significantly affected by exposure to both compounds. The evaluation of the spectral profiles revealed that the nervous-system-specific metabolite *N*-acetylaspartate (NAA), amino acid neurotransmitters (e.g., glutamate, glutamine, GABA, glycine), pyroglutamic acid, unsaturated fatty acids, and choline-based compounds are discriminant biomarkers. Additionally, metabolic changes varied as a function of age, but importantly not of sex.

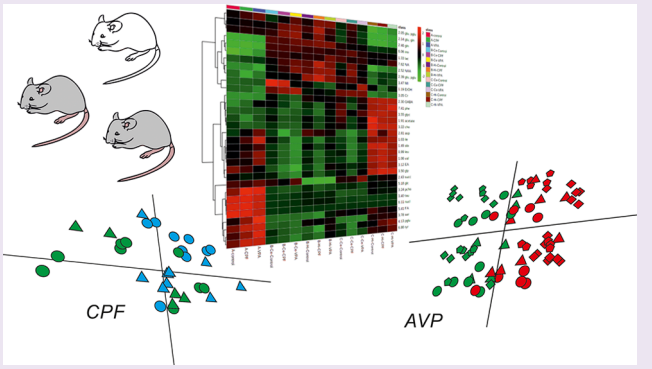

Autism spectrum disorders (ASD) are a heterogeneous group of neurodevelopmental disorders characterized by the absence of or deficits in social interaction and social and verbal communication along with the presence of repetitive, restricted, and stereotyped patterns of interests and/or behaviors.[1] The origin of ASD is largely unknown; while initial studies suggested a strong genetic heritability of autism, recent studies have demonstrated an equally strong role for environmental risk factors.[2,3] Indeed, environmental chemical exposures, such as airborne pollution and pesticides, are increasingly understood to be important contributors to autism. Current theories pose that autism is caused by the dynamic relationship between multiple genetics, environmental factors, and epigenetic mechanisms. This combination of variables may disrupt the normal processes of nervous system development, interfering with neuron formation and migration, synapse formation, and neurological connectivity, and render vulnerability to autism and other neurodevelopmental disorders.[4]

Valproic acid (VPA) is an antiepileptic drug with teratogenic potential that can be prescribed to pregnant women. Prenatal exposure to VPA has been linked to a greater occurrence of ASD in humans.[5] It was demonstrated that VPA forms a developmental switch that modulates synapse maturation and functions by inhibiting histone deacetylases HDAC1 and HDAC2 in immature and mature neurons,[6] causing a robust facilitation of excitatory synapse maturation and a modest increase in synapse numbers, which may be associated with behavioral deficits observed in ASD.[7]

Organophosphorus pesticides, among which is chlorpyrifos (CPF), are widely distributed environmental toxicants associated with neurobehavioral deficits and an increased risk of ASD occurrence in children.[8] Evidence has been accumulated over the past decade showing that noncholinergic mechanisms may play a role in the neurotoxic effects of CPF exposure in rodents, involving disruption of neural cell development, neurotransmitter systems, and synaptic formation and metabolism in different brain regions.[9,10] Such developmental disruptions have been associated with later functional impairments in behavior, learning and memory,

Received: January 27, 2021
Accepted: March 8, 2021
Published: March 17, 2021

https://doi.org/10.1021/acschembio.1c00053
ACS Chem. Biol. 2021, 16, 753–765

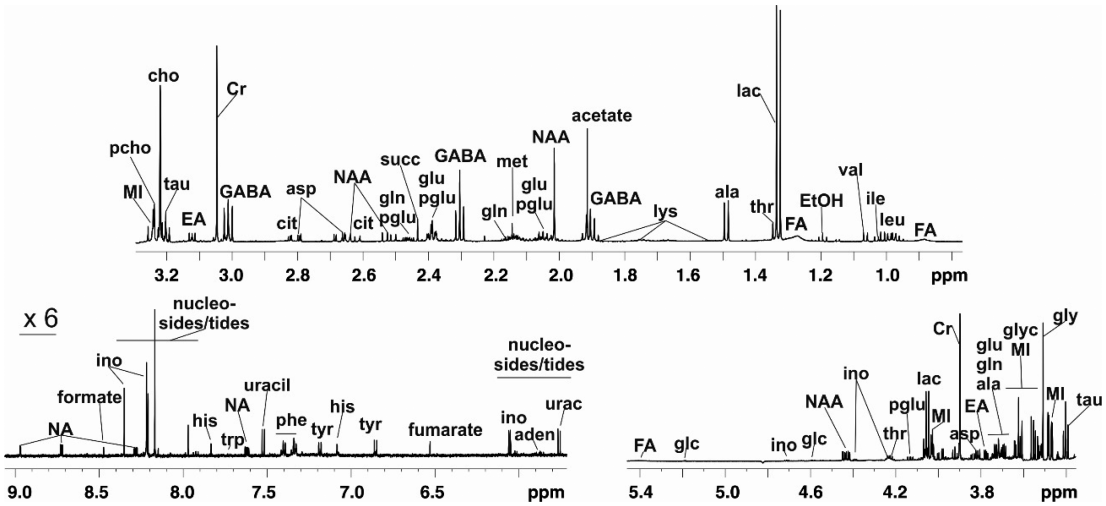

Figure 1. Subregions of a typical ^{1}H NMR spectrum (600 MHz) of the CD_3OD/D_2O KH_2PO_4 buffer (80:20, v/v) extract of the left side of the hippocampus tissue taken from a male adult rat from the control group. Abbreviations: aden, adenosine; ala, alanine; asp, aspartate; cho, choline; cit, citrate; Cr, creatine; EtOH, ethanol; EA, ethanolamine; FA, fatty acids; GABA, α-aminobutyrate; glc, glucose; gln, glutamine; glu, glutamate; gly, glycine; glyc, glycerol; his, histidine; ile, isoleucine; ino, inosine; lac, lactate; leu, leucine; lys, lysine; met, methionine; MI, *myo*-inositol; NAA, *N*-acetylaspartate; NA, niacinamide; pcho, phosphocholine; pglu, pyroglutamate; phe, phenylalanine; ser, serine; succ, succinate; tau, taurine; thr, threonine; trp, tryptophan; tyr, tyrosine; val, valine.

gene expression, and the gut microbiome.[11−14] In addition, the developmental exposure to low doses of CPF has been also associated with an ASD-like phenotype concerning both social and communicative behaviors in mice models.[15,16] Recently, we have shown a reduction in ultrasonic vocalizations at postnatal day 7 of rat pups prenatally exposed to either VPA or CPF, indicative of communicative deficits similar to ASD.[17] This is relevant as the characteristics and regulation of social outcomes in rats are more "similar" to humans than those observed in mice.[18]

Identification of biomarkers is always a challenge considering the complexity and diversity of molecular pathways implicated in most neurological disorders. Among the new omics, metabolomics has the potential to gain a deeper understanding of many complex diseases and genetic−environment−health paradigms. By providing a global study of low molecular weight metabolites (<1500 Da) in biofluids (plasma/serum and urine) and tissues, metabolomics assures the characterization of an individual metabolic phenotype that permits the detection of rapid biochemical pathway alterations and unravels multiple biomarker panels.[19] Identification of biomarkers is critical for disease research. Their detection can be used for risk assessment (directed at the potential for primary prevention), screening (for early detection and early intervention of disease), to diagnose or stage diseases, and also to evaluate and monitor treatment effects.[20] For example, metabolomics tools are being intensively applied with the aim of obtaining cancer-associated biomarkers that would monitor the metastatic state or the therapeutic and drug responses.[21] Moreover, biomarkers may serve as novel targets for drug therapy and may even be used in precision medicine.[22]

In this study, we aimed to explore brain metabolic changes in a rat model of ASD induced by prenatal exposure to VPA. Two additional groups were added to the study, one exposed to CPF and another exposed only to the CPF vehicle (DMSO).[17] We compared the effects of CPF and VPA exposure in both male and female rats at different postnatal ages in the metabolome of different tissues of the brain (hippocampus and cerebellum). Cerebellar and hippocampus disfunctions have been strongly correlated with several imbalances in ASD human and animal models,[23−26] and therefore, these two brain regions were the ones studied herein. The biochemistry in these two anatomical regions is expected to be disturbed to different extents by the administration of these xenobiotics. We hypothesized that prenatal exposure to VPA and CPF will induce different metabolic changes as a function of age and sex. Although male predominance in ASD is well-known, the neurobiological mechanism underlying the male predominance is not clear yet.[7] Interestingly, while a 4:1 male/female ratio is observed in the human ASD population,[27] the male/female ratio in children prenatally exposed to VPA who develop ASD is 1:1.[28]

The metabolomic analysis was achieved using an analytical platform based on a liquid high-resolution NMR spectrometer equipped with a high-sensitivity cryoprobe, which is the method of choice for efficient quantification of tissue metabolites. NMR spectroscopy gives immediate qualitative and quantitative information on around 10^2 different small molecules present in a biological sample, without *a priori* selection of specific biochemical pathways, thus enabling a broad unbiased approach.[29] Additionally, NMR allows a high-throughput analysis and high reproducibility, and it is an intrinsically quantitative technique over a wide dynamic range, thanks to the linear response of NMR signals within concentration, and with the use of just one internal reference compound.[30]

RESULTS AND DISCUSSION

Metabolite Profiling of Mice Brain Samples. Figure 1 displays a labeled ^{1}H NMR spectrum of a representative CD_3OD/D_2O KH_2PO_4 buffer (80:20, v/v) extract obtained from the hippocampus of an adult control group. Table S1 shows information on metabolite assignments. The ^{1}H NMR spectra contained a large number of prominent resonances assignable to a wide range of metabolites involved in a broad association of metabolic pathways that are common to

https://doi.org/10.1021/acschembio.1c00053
ACS Chem. Biol. 2021, 16, 753−765

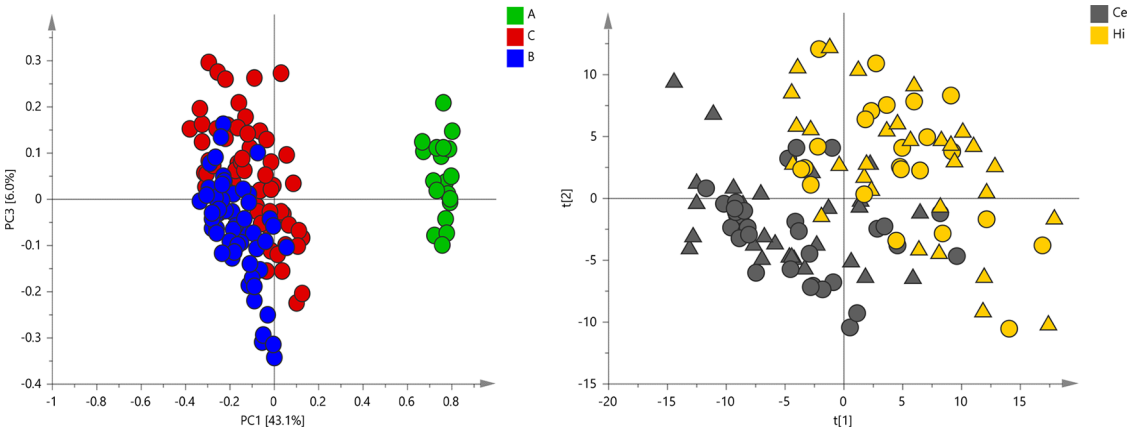

Figure 2. Metabolic alterations driven by aging and across different brain regions. (A) Principal component analysis (PCA) scores plot of PC1/PC3 (PC1/PC2 is shown in Figure S7) obtained from ^{1}H NMR data and colored according to the age of the population [group A, neonatal (PND1); group B, adolescent (PND47−48); group C, adult (PND202−206)]; scaling was done to Pareto. (B) Partial least squares discriminant analysis (PLS-DA) scores plot from ^{1}H NMR spectra of extracts from left (○) and right (Δ) parts of the hippocampus (Hi, yellow scores) and cerebellum (Ce, gray scores) from teens and adults; scaling was done to unit variance; R^2 = 0.815, Q^2 = 0.853, CV-ANOVA = 2.38 × 10^{-36}. Loadings plots explaining both discriminations can be found in Figures S2 and S3.

mammalian cells (e.g., amino acids, branched-chain organic acids, polyols, phospholipids, and metabolites associated with energy metabolism, glycolysis, etc.) and others that are brain-specific. Important metabolites include the neuron marker *N*-acetylaspartate (NAA), a key link between distinct biochemical features of CNS metabolism; glutamate (Glu), glutamine (Gln), and α-aminobutyrate (GABA), amino acid neurotransmitters that interact through the Glu/GABA-Gln cycle to maintain cortical excitation/inhibition equilibrium; myo-inositol (MI), a major osmolite precursor for phosphoinositides involved in the second messenger system; taurine (Tau), involved in neuronal excitability, synaptic potentiation, and osmoregulation; and choline (Cho)-based compounds, essential components of cellular membranes and necessary for the synthesis of the neurotransmitter acetylcholine. Compared with other organs, the brain contains the largest diversity of lipid molecular species. Broad signals from fatty acids (FAs) were observed in the ^{1}H NMR spectra, which according to the literature may belong to arachidonic acid (ω-6), docosahexaenoic acid (ω-3), linoleic acid (ω-6), oleic acid (ω-9), saturated FA palmitic acid, and stearic acid, among others.[31]

Metabolic Alterations Driven by Aging and Across Different Brain Regions. Different tissues of the brain (left and right sides of hippocampus and cerebellum) were analyzed for both male and female rats at different postnatal ages (group A, neonatal (PND1); group B, adolescent (PND47−48); and group C, adult (PND202−206)) together with the control VPA- and CPF-exposed groups. For neonatal rats, brains were not separated by regions due to their small size and were analyzed intact. An exploratory analysis of the ^{1}H NMR spectra from all brain extracts was first made using a principal component analysis (PCA) technique to reveal the main trends in our ^{1}H NMR data set. The PC1/PC3 scores plot of Figure 2a reveals a clear separation of neonatal intact brain samples from brain regions of older groups (B and C). The analysis of the discriminant metabolites by the application of a PLS-DA to the ^{1}H NMR data set (Figure S1) allowed the conclusion that neonatal intact brains showed a higher concentration of nucleotides, cofactors, Tau, glucose (glc), and choline-based metabolites [Cho and phosphocholine (Pcho)] compared to the hippocampus and cerebellum regions of teen and adult groups, which in turn showed an increase in GABA, NAA, niacinamide (NA), lactate (Lac), Glu, and uracil. Interestingly, NAA generally increases with neuronal maturation and is an indicator for adult-type neurons and axons. The metabolic changes between specific brain parts from teen and adult groups (B vs C) were also investigated by the application of PLS-DA models to ^{1}H NMR data (Figure S2). A clear discrimination was evident, and many of the assigned metabolites changed significantly with aging: a decrease in Gln, Glu, NAA, Tau, creatine (Cr), and aspartate (Asp) was observed in both brain regions, while the levels of unsaturated fatty acids (UFA), glycerol (Glyc), glycine (Gly), Cho, and GABA increased in the hippocampus (and only the first two in the cerebellum). Some of these metabolic changes associated with the aging effect on the brain metabolome agree with the findings reported from other authors.[32−34]

The metabolic differences between left and right parts of the cerebellum and hippocampus were also investigated by the application of a PLS-DA model (Figure 2b). A clear separation between hippocampus and cerebellum tissues was observed, but no significant differentiation was proved between left and right parts, neither for the hippocampus nor for the cerebellum. Analysis of the discriminant metabolites (in the loadings plot of Figure S3) revealed similar metabolite changes responsible for the clustering between the hippocampus and cerebellum regions for both adults and teens: higher concentrations of GABA, serine (Ser), choline-based compounds (Cho and Pcho), Tau, and Asp were detected in the hippocampus on both adults and teens relative to the cerebellum, whereas Cr, Gln, and succinate (Succ) decreased. Considering the metabolic similarity between the right and left parts of both the hippocampus and cerebellum, these will be analyzed together in the next sections of the manuscript.

Metabolic Alterations in VPA-Exposed Rats. Metabolic changes between the VPA-exposed and the control groups were first investigated individually for neonatal, adolescent, and adult rats in order to remove misleading effects of aging that could mask metabolic changes associated with the drug exposition. For this, OPLS-DA models were applied to the different ^{1}H NMR data sets. Figure 3 shows the application of

https://doi.org/10.1021/acschembio.1c00053
ACS Chem. Biol. 2021, 16, 753−765

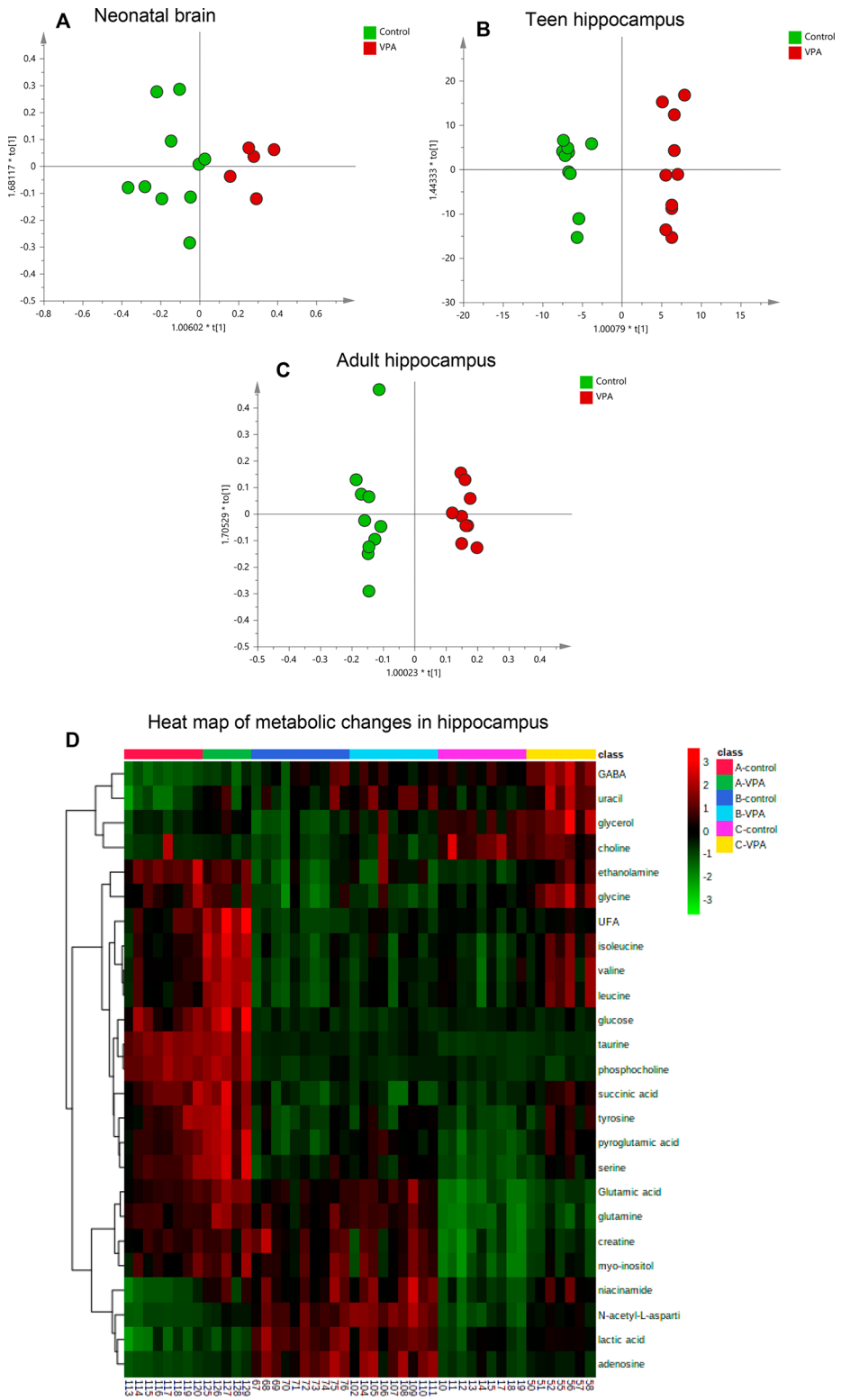

Figure 3. Metabolic alterations in VPA-exposed rats. (A, B, C) Orthogonal partial least squares discriminant analysis (OPLS-DA) score plots that discriminate the effect of VPA prenatal administration from control groups on ^{1}H NMR spectra of extracts in neonatal brains (A, $R^2X = 0.847$; $Q^2 = 0.604$, CV-ANOVA = 0.047), teen hippocampus (B, $R^2X = 0.879$; $Q^2 = 0.901$, CV-ANOVA = 1.6×10^{-4}), and adult hippocampus (C, $R^2X = 0.918$; $Q^2 = 0.792$, CV-ANOVA = 0.030). Colored S-lines showing the metabolite variations that significantly contributed to the discrimination between the classes can be found in Figure S4. (D) Heat map of the most relevant metabolites (with a variable importance in projection (VIP) > 1) from neonatal (group A) intact brains and hippocampus tissues of teen (group B) and adult (group C) rats that were associated with the discrimination between control and VPA-exposed groups. Rows: quantification values of metabolites with VIP > 1. Columns: hippocampus samples from different groups. Color scale indicates metabolites concentration values ranging from green (the lowest) to red (the highest).

https://doi.org/10.1021/acschembio.1c00053
ACS Chem. Biol. 2021, 16, 753−765

Table 1. Summary of the Metabolic Changes Observed in Neonatal Intact Brains (Group A) and in VPA-Treated Hippocampus and Cerebellum Teen (Group B) and Adult (Group C) Rats

		VPA-exposed rats									
		intact brain		hippocampus				cerebellum			
		A vs control		B vs control		C vs control		B vs control		C vs control	
metab.	ppm	FC[a]	p value[b]	FC[a]	p value[b]	FC[a]	p value[b]	FC[a]	p value[b]	FC[a]	p value[b]
NAA	2.52	1.30	4.0×10^{-4}	1.20	0.0016	1.61	7.8×10^{-4}			1.37	0.023
Glx	2.46	1.23	0.025	1.20	0.025	1.36	8.4×10^{-4}			1.36	0.026
Pglu	4.13	1.36	0.009	1.31	0.002	1.61	3.8×10^{-4}			1.29	0.038
uracil	5.76	1.76	0.023	1.32	0.019	1.60	0.002				
UFA	5.41	2.14	0.004	1.85	0.003	1.22	0.005				
Asp	2.81	1.43	0.008			1.23	0.037			1.27	0.027
Ile	1.03	1.67	0.004			1.54	0.011	−1.33	0.003		
Glyc	3.55	1.26	0.011			1.32	0.024	−1.30	0.042		
Ser	3.78	1.29	0.031			1.38	0.006				
Tyr	6.86	1.30	0.046			1.50	0.020	−1.27	0.014	−1.18	0.042
Phe	7.41	1.52	0.007			1.48	0.015	−1.36	1.3×10^{-4}		
NA	7.62	1.58	0.009			1.42	0.003				
Lac	1.33	1.26	0.040			1.19	0.011				
MI	3.47					1.33	0.002				
Cr	3.05					1.30	0.004				
Tau	3.40					1.33	0.002				
Ala	1.49					1.31	0.027	−1.24	0.030		
Succ	2.43					1.59	0.001				
Gly	3.51					1.41	0.001	−1.39	0.014		
GABA	2.30					1.24	0.025	−1.34	0.017	1.36	0.026
Val	1.06	1.47	0.011					−1.33	0.003		
Glc	5.18	1.55	0.041					−1.36	0.015	−1.32	0.009
Cho	3.22							−1.45	0.013	−1.31	0.038

[a]Fold change (FC) between VPA-exposed rats and controls. FC with a positive value indicates a relatively higher concentration present in VPA-exposed rats, while negative values mean a relatively lower concentration as compared to the normal control. [b]FCs were calculated for metabolites showing statistically significant changes between the two groups: p values < 0.05 using ANOVA followed by Fisher's least significant difference (LSD) post hoc test and q (FDR) < 0.05 validation from generated volcano plots via the Metaboanalyst software. Abbreviations: ala, alanine; asp, aspartate; cho, choline; Cr, creatine; GABA, α-aminobutyrate; glc, glucose; glx, glutamine + glutamate; gly, glycine; glyc, glycerol; ile, isoleucine; lac, lactate; MI, *myo*-inositol; NA, niacinamide, NAA, *N*-acetylaspartate; pcho, phosphocholine; pglu, pyroglutamate; phe, phenylalanine; ser, serine; succ, succinate; tau, taurine; tyr, tyrosine; UFA, unsaturated fatty acids; val, valine.

OPLS-DA model score plots for (a) neonatal brains and for the hippocampus of (b) teens and (c) adults, showing clear discrimination between VPA groups and controls. Analysis of the loadings, represented by S-line plots, revealed the significant class-discriminating NMR regions responsible for the clustering patterns (Figure S4). The panel of metabolites with a variable importance in projection (VIP) > 1 from OPLS-DA models was quantified, in order to avoid misinterpretation of the discriminant metabolites due to overlapping signals in the discriminant loadings and was used to generate the heat map of Figure 3d, using the Pearson correlation and the average linkage method. The generated heat map allows for a better visualization of all hippocampal metabolic alterations caused by the prenatal administration of VPA.

In the cerebellum, the application of the OPLS-DA model only found a statistically valid discrimination for teens (Figure S5). A heat map displaying the metabolic content of the cerebellum from VPA-exposed and control rats was also generated and can be found in Figure S5.

The panel of discriminant metabolites identified to statistically changed between VPA-exposed and control rats in the two brain regions are summarized in Table 1. Some of these metabolites are involved in the key metabolic pathways, including neurotransmitters (Glu, Gln, GABA, Asp, Gly), mitochondrial metabolism (NAA), UFA, energy metabolism (Glc, Lac, Cr), membranes (MI, Cho, Pcho), amino acids, etc. As expected, VPA caused significant disturbances in the endogenous metabolite profiles, especially in the hippocampus, which plays an important role in learning, memory, and cognitive function. In fact, much data from human and animal models show a clear implication of hippocampus in ASD, i.e., excitation/inhibition imbalance due to GABAergic interneuron defects.[35,24,36]

Metabolic brain perturbations imposed by VPA were detected as early as in neonatal rats, in which 16 metabolites were found to differ between control and VPA-exposed groups. With aging, most of these metabolic changes were also observed in the adult hippocampus together with some others, but fewer were detected in teens. Lesser changes during adolescence are probably a reflection of developmental programs that are age dependent. For instance, schizophrenia's main symptoms do not appear until late adolescence or early adulthood, despite the neurobiological causes initiating prenatally.[37] In addition, adolescence is a period of multiple physiological changes, especially in the neuroendocrine system, making metabolic activity very distinct between teens and adults.[38] Only six metabolites showed a consistent increase between VPA and control groups for the neonatal brain and for both the teen and adult hippocampus: NAA, Glu, and Gln (referred collectively as "Glx"); pyroglutamate (pglu, the cyclic

https://doi.org/10.1021/acschembio.1c00053
ACS Chem. Biol. 2021, 16, 753−765

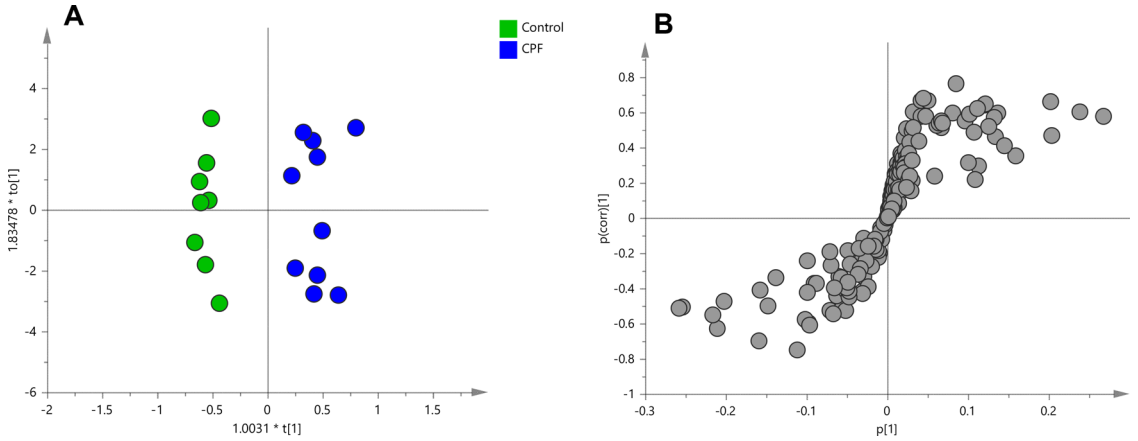

Figure 4. Orthogonal partial least squares discriminant analysis (OPLS-DA) scores plot (A) and S-plot (B) that discriminate the effect of CPF prenatal administration on ^{1}H NMR spectra from control groups in adult hippocampus (R^2 = 0.956; Q^2 = 0.742, CV-ANOVA = 0.022). The main spectral regions with a variable importance in projection VIP superior to 1 were the following: NAA (loadings 2.68, 2.54, 2.50, 2.02, 4.42), pyroglutamate (2.04, 2.48, 4.14), GABA (loadings 1.90, 2.30, 3.02), succinate (loading 2.42), which increased in the CPF-exposed group, while unsaturated fatty acids (loading 5.40, 1.26, 1.30, 1.34, 0.96) increased in the control group.

Table 2. Summary of the Metabolic Changes Observed in CPF-Exposed Adolescents (Group B) and Adults (Group C) Brains

		CPF-exposed rats							
		hippocampus				cerebellum			
		B vs control		C vs control		B vs control		C vs control	
metab.	ppm	FC[a]	p value[b]	FC[a]	p value[b]	FC[a]	p value[b]	FC[a]	p value[b]
NAA	2.52	1.20	0.010	1.33	0.034	1.27	0.041	1.54	0.002
Glx	2.46	1.17	0.042			1.25	0.045	1.64	9.1×10^{-4}
Pglu	4.13			1.33	0.016				
UFA	5.41	−1.42	0.002	−1.32	0.012				
GABA	2.30			1.23	0.043	−1.34	0.003	−1.35	0.039
Gly	3.51	−1.3	0.004			−1.26	0.019	−1.42	0.029
Glyc	3.55	−1.2	0.034					−1.39	0.013
Cho	3.22					−1.33	0.042	−1.36	0.048
Acet						−1.23	0.040		
Glc	5.18								
Succ				1.40	0.006				

[a]Fold change (FC) between CPF-exposed rats and controls. FC with a positive value indicates a relatively higher concentration present in CPF-exposed rats, while negative values mean a relatively lower concentration as compared to the normal control. [b]FCs were calculated for metabolites showing statistically significant changes between the two groups [p values < 0.05 using ANOVA followed by Fisher's least significant difference (LSD) post hoc test and q (FDR) < 0.05) validation from generated volcano plots via the Metaboanalyst software. Abbreviations: acet, acetate; cho, choline; GABA, α-aminobutyrate; glc, glucose; glx, glutamate + glutamine; gly, glycine; glyc, glycerol; NAA, N-acetylaspartate; pglu, pyroglutamate; succ, succinate; UFA, unsaturated fatty acids.

lactam of glutamic acid); uracil; and UFA. Additionally, in the neonatal and in the adult hippocampus, an increase on several amino acids (isoleucine, serine, tyrosine, phenylalanine), Lac, Asp, and NA was detected.

In the cerebellum, NAA, Glx, Pglu, GABA and Asp levels also increased for adults, as they did in the hippocampus. Moreover, the content of Cho (marker for membrane integrity), tyrosine, and glucose decreased in the cerebellum with VPA administration for both adolescents and adults. Cerebellar metabolic alterations in VPA-exposed adolescents also showed a decrease in the levels of other amino acids besides tyrosine (phenylalanine, valine, alanine, glycine, and isoleucine) and also glycerol.

Metabolic Alterations in CPF-Exposed Rats. Concerning CPF exposure, CPF has been linked to important alterations in metabolites that are related to intermediate cell energy production, amino acid metabolism, as well as glucose and lipid metabolism.[14] OPLS-DA models were applied to NMR spectra from CPF-exposed and control groups, and valid discriminations among them were obtained in the adult hippocampus (Figure 4) and in the cerebellum of both teens and adults (Figure S6). For neonatal pups exposed to CPF, since the number of pups obtained was very low, we did not consider this group in the statistical analysis. The discriminant metabolites (with VIP > 1) were quantified, and statistically significant fold-changes of their concentrations among CPF-exposed and control groups are summarized in Table 2 for the two brain regions.

Metabolic perturbations imposed by exposure to low doses of CPF were fewer than those caused by VPA, implying that CPF prenatal administration caused fewer perturbations in the brain metabolic routes than VPA. Nevertheless, some metabolic changes were similar between CPF and VPA exposition. CPF-exposed groups also showed a general increase

https://doi.org/10.1021/acschembio.1c00053
ACS Chem. Biol. 2021, 16, 753−765

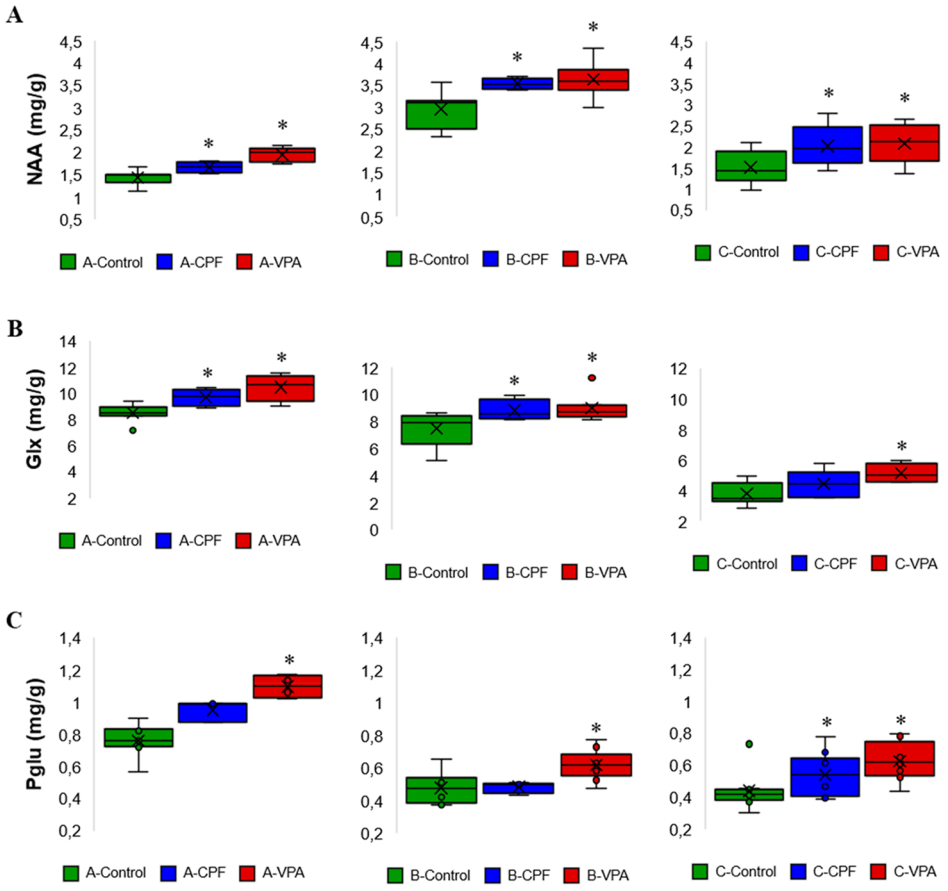

Figure 5. Box plots showing the concentration ranges (mg per gram of dry sample), median quartiles, and extremes for (A) NAA, (B) Glx (glutamate + glutamine), and (C) pyroglutamate for neonatal (class A) intact brains and teen (group B) and adult (group C) hippocampus from the control and VPA- and CPF-exposed rats. *$p < 0.05$ using ANOVA analyses followed by the least significant difference (LSD) post hoc tests.

in NAA, Glx, and pyroglutamate (only in the hippocampus), accompanied by a decrease in the content of glycine and choline (only in the cerebellum) and also of glycerol, acetate, and UFA (only in the hippocampus).

Overview of the Main Metabolic Changes with VPA and CPF Exposition. Our results suggest that NAA suffered a general increase with prenatal exposure to VPA and CPF in both the hippocampus and cerebellum for all age groups. NAA is employed as a general indicator of neuronal health, and specifically mitochondrial function. Contrarily to what we observed, reduced levels of NAA seem to be associated with ASD and to neurofunctional abnormalities.[39] Besides NAA, the literature shows an association of autism with decreased Cr, choline-based compounds, ans MI and with increased Glu and Gln ("Glx") levels.[40] However, there is a great deal of inconsistency between studies and methodologies applied and a lack of discussion about the complexity of interactions within and between the metabolic pathways, which is of particular importance in the development of the theoretical framework associated with ASD. In agreement, our results also indicate that Glx (Glu/Gln) levels were consistently increased across the two brain regions in all age groups, after administration of VPA and CPF compared to the control. The increment in Glx for VPA- and CPF-treated rats was not always accompanied by an increase in GABA. GABA is the major inhibitory neurotransmitter in the cortex, responsible for halting excitatory glutamatergic activity, so naturally, disruption to either of these metabolites will affect the other. This finding indicates a perturbation in neurotransmitter recycling/production in terms of the changes in the concentrations of Glu, Gln, and GABA and the balance between the excitatory and inhibitory neurotransmitters glutamate and GABA, respectively. An impaired glutamate/GABA-glutamine cycle has been linked to ASD related phenotypes and behavior.[41,42] Ford et al.[43] reported that increased anterior cingulate Glx has been related to more negative ASD symptoms and to social and communication deficits. Other authors reported an elevated concentration of Glu in the serum of ASD individuals, as well as for glycolysis products, such as lactate,[44,45] and reduced GABA concentration.[46,47] In our case, an increase in lactate was also observed in VPA-exposed adult hippocampus and neonatal brains, and a reduction on GABA was mostly observed in the cerebellum of VPA- and CPF-exposed groups. Moreover, concentrations of pyroglutamic acid were also found to increase, especially in VPA-exposed brains. Pglu is involved in glutamate storage and acts in the γ-glutamyl cycle (GGC) to regulate the concentration of cerebral glutamate, toxic to the brain at very low concentrations. Also, Pglu is believed to be associated with the production of two other important neurotransmitters (GABA and glycine). Figure 5 shows the box-and-whisker plots of NAA, Glx, and pglu concentrations in neonatal brains and in the teen and adults hippocampus from control and VPA- and CPF-exposed groups, with an indication of the concentration ranges, median quartiles, and extremes.

https://doi.org/10.1021/acschembio.1c00053
ACS Chem. Biol. 2021, 16, 753−765

In the hippocampus, a general increase in total UFA was detected in VPA-treated rats, while it decreased in CPF-exposed rats. Lipids are essential factors in neural development and have critical roles in neuronal migration, differentiation, morphogenesis, myelination, memory formation, and synaptic plasticity, which are highly relevant to ASD.[48] In particular, polyunsaturated fatty acids (PUFAs), such as omega-3 and -6 PUFAs, play a critical role in the structure and function of the neuronal cell membranes in the brain, as well as in the development and homeostasis of the retina and myelin sheath, and perturbations in their content have been implicated in ASD.[49] El-Ansary et al.[50] detected increases in saturated FAs (such as stearidonic acid) as well as decreases in PUFAs (such as eicosapentaenoic acid, docosahexaenoic acid, and arachidonic acid) in ASD children. Thus, further studies investigating lipid profiles, especially the ratio n-3/n-6, using other analytical platforms are necessary since they may help to uncover our understanding of biological mechanisms of ASD and explain the opposite results obtained with VPA and CPF exposure. Also, some studies suggest that n-3 DHA deficiency alters GABAergic activity so it would be interesting to study the correlation between omega n-3 brain levels and Glu/GABA-Gln levels.

Finally, choline-based compounds and glycine were shown to decrease with VPA and CPF exposure in the cerebellum of both teens and adults. Box plot representations of the concentrations of choline and glycine in the cerebellum of VPA- and CPF-exposed teen and adult rats together with their controls can be found in Figure 6. Likewise, cholinergic pathways have been linked to social and behavioral abnormalities, particularly in ASD symptom severity. In this line, Ford and Crewther[40] have reviewed several studies relating choline concentrations in ASD and concluded that choline is typically reduced in children diagnosed with ASD

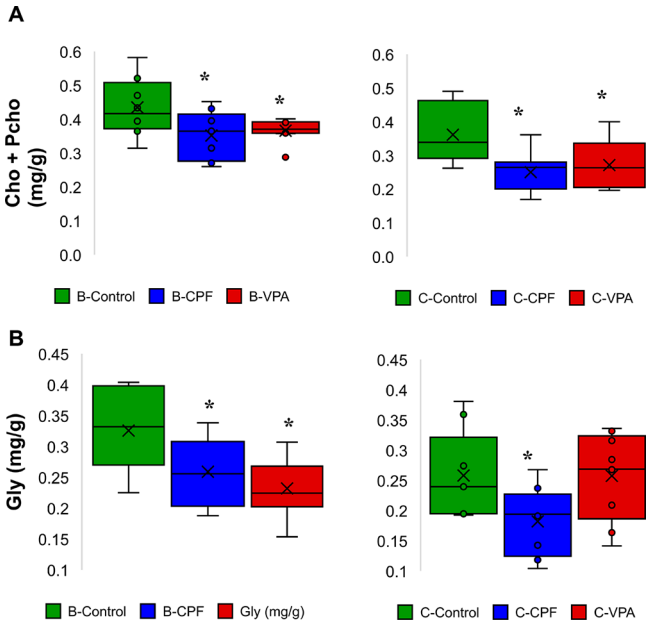

Figure 6. Box plots showing the concentration ranges (mg per gram of dry sample), median quartiles, and extremes for (A) choline-based compounds (Cho+ Pcho) and (B) glycine from the cerebellum of teens (group B) and adults (group C) from the control and VPA- and CPF-exposed groups. *$p < 0.05$ using ANOVA analyses followed by the least significant difference (LSD) post hoc tests.

and increased during adulthood. Choline and glycine are interrelated through their roles in methyl metabolism: choline is metabolized to betaine, which donates a methyl group to homocysteine to form methionine, also generating dimethylglycine, which is further metabolized to glycine. Glycine is the simplest amino acid with a number of functions including fat metabolism, neurological function, muscle development, and incorporation into the antioxidant glutathione.[51] Dysregulations of glycine among other amino acids in ASD were also found by some authors.[51−53]

Finally, to understand if the sex contributed to the discrimination between VPA-treated and control groups, i.e., to unravel if this discrimination was more relevant for a specific sex, OPLS-DA models were applied to the different data sets. No valid models were obtained that could discriminate metabolic changes individually for control and VPA- and CPF-control groups for any brain region or age, suggesting that the discrimination between VPA-treated and control groups was not enhanced for any particular sex. Accordingly, the male/female ratio in children prenatally exposed to VPA who develop ASD is 1:1, contrary to the 4:1 male/female ratio observed in human ASD population.[27,28] Nevertheless, future studies employing a larger number of replicates would be necessary.

Quantitative Network Metabolic Pathway Analysis. The obtained metabolite profiles not only represent discrete sets of small molecule biomarkers but they can be organized into consistent and statistically robust metabolite parameters characteristic of specific metabolic pathways being activated. Figure 7 shows a summary of some metabolic pathways that might be disturbed due to changes in the levels of the above-mentioned metabolites due to VPA and CPF exposure.

Furthermore, Figure 8 shows statistically significant VPA-induced modulations to a series of metabolic pathways in the adult hippocampus obtained by a quantitative network pathway analysis involving pathway enrichment analysis and pathway impact from pathway topology. Pathways were considered significantly enriched if the Holm p value (adjusted by Holm-Bonferroni method) and false discovery rate (FDR)-adjusted p values were lower than 0.05; the profiled metabolites (hits) relative to the total metabolites of the pathway (match status) are higher than 1; and the impact score (indicating the impact of significantly affected metabolites in the pathway based on network topology measure of relative betweenness centrality) is higher than 0. Values of impact, p-values, and Holm adjusted p values for relevant metabolic pathways are described in Table S2.

As can be observed in Figure 8, several biochemical pathways were affected by VPA prenatal exposure in the adult hippocampus (hits > 1, impact > 0, Holm and FDR adjusted $p < 0.05$). Pathways in bold were also found to be statistically altered in neonatal rats. These included the metabolisms of "alanine, aspartate, and glutamate," "arginine and proline," "butanoate," "glutathione," "glyoxylate and dicarboxylate," "D-glutamine and D-glutamate," and "phenylalanine" and the biosynthesis of "aminoacyl-tRNA," "arginine," and "phenylalanine, tyrosine, and tryptophan," which were deemed statistically significant for both adults and the neonatal. In the adult hippocampus, the TCA cycle was also shown to be affected by VPA exposure, which is in accordance with the analysis of the disturbed metabolic pathways described in Figure 7. Regarding CPF effects in the cerebellum, metabolic changes did not meet all the selected criteria, since

https://doi.org/10.1021/acschembio.1c00053
ACS Chem. Biol. 2021, 16, 753−765

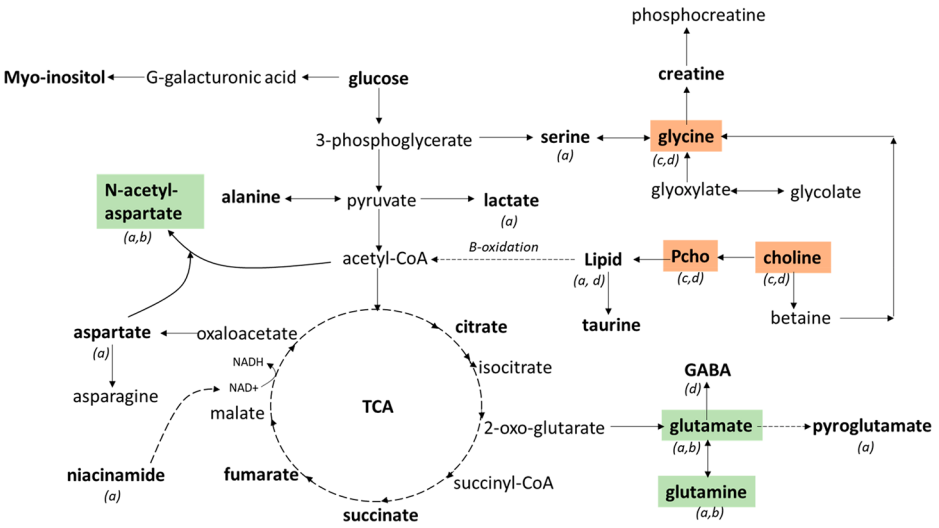

Figure 7. Disturbed metabolic pathways of the most relevant metabolites between VPA- and CPF-exposed rats and control rats. Metabolites that were visualized in the NMR spectra are highlighted in bold. (a) Metabolites that generally increased with VPA exposure in the hippocampus and cerebellum (for at least two group ages); (b) metabolites that generally increased with CPF-exposure in the hippocampus and cerebellum; (c) metabolites that generally decreased in the cerebellum or hippocampus with VPA exposure; (d) metabolites that generally decreased in the cerebellum or hippocampus with CPF exposure. Common changes among VPA and CPF exposure are highlighted in green (for increments) and orange (for reductions).

metabolic routes with a number of hits superior to one were not statistically significant.

Pathway analysis suggested major changes in nitrogen metabolism since the pathways most impacted by VPA exposure involved amino acids and other nitrogen-containing metabolites. In fact, previous studies showed that autistic spectrum disorders come from a family background of dysregulated amino acid metabolism.[54] Tărlungeanu et al.[55] identified a form of ASD resulting from a failure of the brain to properly import amino acids. With respect to our results, some amino acids were found to increase with VPA exposure in the hippocampal region of the adult rats (e.g., tyrosine, phenylalanine), while decreasing in the cerebellum. The glutathione metabolism pathway was also found to be significantly altered with VPA exposure in the adult hippocampus and neonatal brains. This is in accordance with the alterations observed in the level of glycine, which is incorporated into glutathione. Glutathione plays important roles in antioxidant defense, nutrient metabolism, and regulation of cellular events and its deficiency contributes to oxidative stress, which plays a key role in aging and the pathogenesis of many diseases (including kwashiorkor, seizure, Alzheimer's disease, Parkinson's disease, etc.).[56]

CONCLUSIONS

Our study has elucidated the complex network of metabolic events in different parts of the brain as a function of normal aging and exposure to CPF and VPA, which may offer new insights into the autism pathophysiology. Unfortunately, because of the genetic complexity of ASD, there is currently no reliable biomarker that can be used to identify children at risk for ASD. The findings of this comprehensive study using an NMR spectroscopy-based metabolomics approach helped us to understand metabolic changes imposed by prenatal exposure to two chemical agents, VPA and CPF, which are associated with an increased risk of ASD occurrence, at different postnatal ages, in different brain tissues and in subjects of both sexes. The results of this study demonstrated that VPA and CPF prenatal exposure may evoke both specific and common metabolic responses in different tissues of the brain, depending on the aging process, but no correlation was found with sex. Concerning the exposure to VPA, changes in some metabolites were common in all group ages: NAA, glutamate, glutamine, and pyroglutamate generally increased with VPA exposure in both brain regions, while unsaturated fatty acids increased in the hippocampus. In the cerebellum, a decrease of choline-based compounds, glycine, glucose, and tyrosine were detected for both teens and adults with VPA exposure. With respect to CPF, its prenatal administration also caused an increase in NAA and Glx levels in both the hippocampus and cerebellum and a decrease in choline-based compounds, GABA, and glycine in the cerebellum. Reduced GABA along with an increase in glutamate and glutamine concentrations might indicate a cortical excitation/inhibition imbalance, which may contribute to the development of ASDs. These observations provided a broad insight for the systemic effects on brain metabolism derived from the exposure to important ASD-inducing chemicals. Further studies are however needed to elucidate the metabolic interactions and specific mechanisms underlying ASD development.

METHODS

Experimental Animals. The experiment was conducted on Wistar rats (Janvier laboratories). Twenty-five pregnant Wistar rats were housed individually in clear polycarbonate cages (50 × 15 × 24 cm) under a reverse 12-h light/dark cycle (lights on from 19:00 h to 07:00 h). Animals were acclimated to their new regulated environment (temperature, 22 ± 2 °C; humidity, 50 ± 10%) for 6 days. On the expected day, dams gave birth (considered as postnatal day 0; PND0). The next day (PND1), all pups were separated from their mothers to be randomly distributed among all of them until there were 10 pups per dam (five females and five males). All dams had free access to food and water. To detect sings of intoxication, we controlled the weight of the pups repeatedly. This procedure started on PND10 to avoid extreme mother reactions which could affect to the pups. This study is part of the project PSI2017-86847-C2-1-R and was conducted in conformity with the Spanish Royal Decree 53/2013

https://doi.org/10.1021/acschembio.1c00053
ACS Chem. Biol. 2021, 16, 753−765

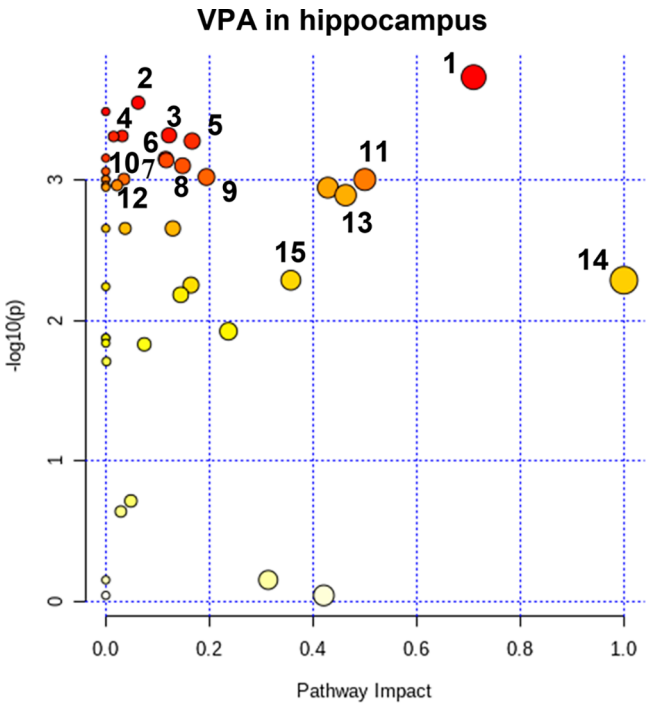

Figure 8. Metabolic pathways significantly affected by VPA exposure in the adult hippocampus (impact > 0, number of metabolite hits in the pathway > 1, Holm and FDR adjusted $p < 0.05$). For the analyses, the quantification values of the selected metabolites were used. 1*, alanine, aspartate, and glutamate metabolism; 2, citrate cycle (TCA cycle); 3*, arginine and proline metabolism; 4*, butanoate metabolism; 5*, aminoacyl-tRNA biosynthesis; 6*, glutathione metabolism; 7*, arginine biosynthesis; 8*, glyoxylate and dicarboxylate metabolism; 9*, nicotinate and nicotinamide metabolism; 10, galactose metabolism; 11*, D-glutamine and D-glutamate metabolism; 12, cysteine and methionine metabolism; 13, glycine, serine and threonine metabolism; 14*, phenylalanine, tyrosine, and tryptophan biosynthesis; 15*, phenylalanine metabolism. Pathways marked with an asterisk "*" were also found to be statistically altered in neonatal rats with VPA exposure. Values of impact, p values, and Holm adjusted p values are described in Table S2.

and the European Community Directive (2010/63/EU) for animal research and approved by the University of Almeria Animal Research Committee.

Protocol of Drug Administration. Following the protocol previously published by Morales-Navas et al.[17] from gestational day 12.5 to 15.5 (GD12.5−15.5), the dams randomly assigned to the CPF group received one subcutaneous injection of 1 mg kg^{-1} of CPF [O,O-diethyl O-3,5,6-trichloropyridin-2-yl phosphorothioate (Pestanal, Sigma-Aldrich)] dissolved in DMSO, each day. The dams randomly assigned to the VPA group received the critical period of valproate exposure to induce autistic symptoms in Sprague−Dawley rats of 400 mg kg^{-1} of VPA[57] dissolved in 0.9% saline for a concentration of 250 mg mL^{-1}, and three daily subcutaneous injections only with saline. The dams randomly selected to the control group received one daily subcutaneous injection of 1 mL kg^{-1} of dimethyl sulfoxide (DMSO) for 4 days. In order to keep the right dosage, all the dams were weighted every day.

Sacrifices and brain extractions: Neonatal pups (PND1; 10 CNT, four CPF, eight VPA) were sacrificed by cervical dislocation, and the whole brain was quickly removed, flash-frozen, and stored at −80 °C. Both the adolescent (PND47−48; 10 CNT, 10 CPF, 10 VPA) and adult rats (PND202−206; 10 CNT, 10 CPF, 10 VPA) were rapidly decapitated, and the whole brain was removed and dissected (cerebellum, dorsal striatum, frontal cortex, hippocampus, and hypothalamus). In this experiment, only the left and right sides of the hippocampus and cerebellum of the teen and adult rats were analyzed. In the neonatal group, we analyzed the whole brain without performing a dissection. The brains were kept at −80 °C until NMR analysis.

Sample Preparation. Frozen brain tissue samples were freeze-dried for 24 h and mortared to a powder. Then, 12 mg was taken and extracted with 0.8 mL of a mixture of 50:50 (v/v) CH_3OH-d_4 and D_2O KH_2PO_4 buffer (pH 6.0) containing the sodium salt of 3-(trimethylsilyl)propionic-2,2,3,3-d_4 acid (TSP, 0.01% w/w) and sodium azide (NaN_3, 90 μM) as an enzyme inhibitor in 1.5 mL sterile Eppendorf tubes. The samples were sonicated for 20 min, mixed for 10 min (600 rpm), and centrifuged (5 min, 13500 rpm). Five-hundred microliters of the supernatants were collected and transferred to oven-dried 5 mm NMR tubes.

NMR Experiments. All ^{1}H NMR experiments were conducted on a Bruker Avance III 600 spectrometer operating at 600.13 MHz and equipped with a 5 mm QCI quadruple resonance pulse field gradient cryoprobe. All experiments were performed at 293 ± 0.1 K and without rotation. ^{1}H NMR spectra were recorded using a presaturation pulse sequence (Bruker 1D noesygppr1d) to suppress the residual water signal via irradiation of the H_2O frequency during the recycle and mixing time delays. The following acquisition parameters were applied: 32 scans and four dummy scans, 64 000 data points, spectral width 20.5 ppm, acquisition time 2.73 s, relaxation delay of 10 s, receiver gain 57, FID resolution of 0.25 Hz, and mixing time of 10 ms. The spectrometer transmitter was locked to the CH_3OH-d_4 frequency. Acquisition and processing of spectra were carried out with TOPSPIN software (Bruker, version 3.6.2). The resulting spectra were automatically phased, baseline-corrected, and calibrated to the TSP signal at 0.0 ppm. ^{1}H−^{1}H correlation spectroscopy (COSY), ^{1}H−^{1}H total correlation spectroscopy (TOCSY), ^{1}H−^{13}C heteronuclear single quantum coherence (HSQC), and ^{1}H−^{13}C heteronuclear multiple bonds coherence (HMBC) spectra were recorded using standard Bruker sequences. A COSY spectrum was obtained with a D1 of 1.5 s, spectral widths (SW) of 7211.54 Hz in both dimensions, and a receiver gain (RG) of 203, and it was processed using the sine window function (SSB = 0.0). The TOCSY spectrum was obtained with a D1 of 1.5 s, SW of 7211.54 Hz in both dimensions, and RG of 203 and processed using the quadratic sine window function (SSB = 2.0). The HSQC spectrum was acquired using a relaxation delay of 1.0 s and a spectral width of 7211.54 Hz in F2 and 34710.77 Hz in F1, and it was processed using the quadratic sine window function (SSB = 2.0). Finally, the HMBC spectrum was also acquired using a relaxation delay of 1.0 s and a spectral width of 7812.50 Hz in F2 and 37730.04 Hz in F1, and it was processed using the quadratic sine window function (SSB = 2.0).

Metabolite Identification and Quantification. NMR signals were identified thanks to information on scalar couplings extracted from ^{1}H−^{1}H COSY, ^{1}H−^{1}H TOCSY, ^{1}H−^{13}CHSQC, and ^{1}H−^{13}C HMBC spectra, and with the help of the BBIOREFCODE 2 database from Bruker, public NMR databases such as COLMAR and HMDB, and the literature.[29,58,59] Quantification of metabolites was achieved through the integrated values of the related peak areas of nonoverlapped signals in relation to the inner standard (TSP).

Statistical Analyses. AMIX 3.9.12 (Bruker BioSpin GmbH) software was used for bucketing NMR spectra with a bucket size of 0.04 ppm. Normalization was done by scaling the intensity of individual peaks to the total intensity recorded in the region from δ_H 0.2 to 10.0 ppm. Regions of δ_H 4.90−4.74 and 3.34−3.28 ppm were removed due to the presence of the residual signals of H_2O and CH_3OH, respectively. NMR bucketed data were used as the input for multivariate data analysis tools, such as principal component analysis (PCA), partial least-squares discriminant analysis (PLS-DA), and orthogonal partial least-squares discriminant analysis (OPLS-DA), to determine the extent of differences between experimental groups and to identify the metabolic features that contribute to their discrimination. Multivariate data analysis was performed using SIMCA-P software (v. 15.0, Umetrics). PCA and OPLS-DA models were scaled to Pareto while PLS-DA scaling was done to unit variance.

https://doi.org/10.1021/acschembio.1c00053
ACS Chem. Biol. 2021, 16, 753−765

The results of the cross validation for PLS-DA models are given by means of cumulative R^2 and Q^2 values. The PLS-DA models were subsequently subjected to permutation tests (with 100 permutations) to establish whether the observed discrimination between the groups was statistically significant (p value < 0.05). The statistical significance of the estimated predictive power of OPLS-DA models was tested using the ANOVA of the cross-validated residuals (cv-ANOVA) test. Heat maps were generated by the Pearson correlation and the average linkage method with the TSP-normalized integral values for several assigned metabolites using the statistical analysis tool of the web interface MetaboAnalyst 4.0.

The loadings containing metabolites important for a predictive model were evaluated by generating the variable importance in projection (VIP) plot. Loadings with VIP scores superior to 1 were considered relevant to the generated PLS-DA and OPLS-DA models. Metabolites contained in these loadings were quantified with respect to the TSP signal. Fold changes for discriminating metabolites between control and experimental groups were calculated. ANOVA (analysis of variance) analyses followed by least significant difference (LSD) *post hoc* tests were employed to determine the significance of differences for the metabolite ratios between groups; p values < 0.05 were considered statistically significant. Finally, metabolic changes with false discovery rate (FDR)-adjusted p values (q values) < 0.05 were considered.

Pathway Analysis. Pathway analysis, which consisted of enrichment analysis and pathway topological analysis, were conducted with the Metabolomics Pathway Analysis (MetPA) feature within MetaboAnalyst, using the global test algorithm for pathway enrichment (adjusted for multiple testing) and relative betweenness centrality to assess metabolite importance. The *Homo sapiens* pathway library was chosen. This approach was also utilized to provide estimates of pathway impact and FDR-adjusted p values. The p values, Holm p values (adjusted by Holm-Bonferroni method), FDR-adjusted p values, and pathway impact indices are shown for each pathway. Pathways were considered significantly enriched if Holm p < 0.05, FDR < 0.05, and impact > 0 and if the number of metabolite hits in the pathway was >1.

■ ASSOCIATED CONTENT

Supporting Information

The Supporting Information is available free of charge at https://pubs.acs.org/doi/10.1021/acschembio.1c00053.

PLS-DA and OPLS-DA loadings and scores plots, heatmaps, full NMR assignments of all the identified metabolites and metabolic pathways (PDF)

■ AUTHOR INFORMATION

Corresponding Authors

Ignacio Fernández − *Department of Chemistry and Physics, Research Centre CIAIMBITAL, University of Almería, 04120 Almería, Spain*; orcid.org/0000-0001-8355-580X; Phone: +34 950214465; Email: ifernan@ual.es

Fernando Sánchez-Santed − *Department of Psychology and Health Research Center CEINSAUAL, University of Almería, 04120 Almería, Spain*; Phone: +34 950214631; Email: fsanchez@ual.es

Authors

Ana Cristina Abreu − *Department of Chemistry and Physics, Research Centre CIAIMBITAL, University of Almería, 04120 Almería, Spain*

Miguel Morales Navas − *Department of Psychology and Health Research Center CEINSAUAL, University of Almería, 04120 Almería, Spain*

Cristian Perez Fernández − *Department of Psychology and Health Research Center CEINSAUAL, University of Almería, 04120 Almería, Spain*

Complete contact information is available at: https://pubs.acs.org/10.1021/acschembio.1c00053

Funding

This research has been funded by the by the State Research Agency (projects RTC-2016-5239-2, CTQ2017-84334-R, and PSI2017-86847-C2-1-R) of the Spanish Ministry of Science, Innovation and Universities and EU FEDER funds. A.C.A. thanks University of Almería for a postdoctoral Hipatia fellowship.

Notes

The authors declare no competing financial interest.

■ REFERENCES

(1) Frye, R. E. (2018) Social Skills Deficits in Autism Spectrum Disorder: Potential Biological Origins and Progress in Developing Therapeutic Agents. *CNS Drugs 32*, 713−734.

(2) Sandin, S., Lichtenstein, P., Kuja-Halkola, R., Larsson, H., Hultman, C. M., and Reichenberg, A. (2014) The Familial Risk of Autism. *JAMA 311*, 1770−1777.

(3) Hallmayer, J., Cleveland, S., Torres, A., Phillips, J., Cohen, B., Torigoe, T., Miller, J., Fedele, A., Collins, J., Smith, K., Lotspeich, L., Croen, L. A., Ozonoff, S., Lajonchere, C., Grether, J. K., and Risch, N. (2011) Genetic Heritability and Shared Environmental Factors Among Twin Pairs With Autism. *Arch. Gen. Psychiatry 68*, 1095−1102.

(4) Kalkbrenner, A. E., Schmidt, R. J., and Penlesky, A. C. (2014) Environmental chemical exposures and autism spectrum disorders: a review of the epidemiological evidence. *Curr. Probl. Pediatr. Adolesc. Health Care. 44*, 277−318.

(5) Cho, H., Kim, C. H., Knight, E. Q., Oh, H. W., Park, B., Kim, D. G., and Park, H.-J. (2017) Changes in brain metabolic connectivity underlie autistic-like social deficits in a rat model of autism spectrum disorder. *Sci. Rep. 7*, 13213−13213.

(6) Akhtar, M. W., Raingo, J., Nelson, E. D., Montgomery, R. L., Olson, E. N., Kavalali, E. T., and Monteggia, L. M. (2009) Histone Deacetylases 1 and 2 Form a Developmental Switch That Controls Excitatory Synapse Maturation and Function. *J. Neurosci. 29*, 8288−8297.

(7) Sailer, L., Duclot, F., Wang, Z., and Kabbaj, M. (2019) Consequences of prenatal exposure to valproic acid in the socially monogamous prairie voles. *Sci. Rep. 9*, 2453.

(8) De Felice, A., Greco, A., Calamandrei, G., and Minghetti, L. (2016) Prenatal exposure to the organophosphate insecticide chlorpyrifos enhances brain oxidative stress and prostaglandin E2 synthesis in a mouse model of idiopathic autism. *J. Neuroinflammation 13*, 149.

(9) Rauh, V., Arunajadai, S., Horton, M., Perera, F., Hoepner, L., Barr, D. B., and Whyatt, R. (2011) Seven-Year Neurodevelopmental Scores and Prenatal Exposure to Chlorpyrifos, a Common Agricultural Pesticide. *Environ. Health Perspect. 119*, 1196−1201.

(10) Qiao, D., Seidler, F. J., Tate, C. A., Cousins, M. M., and Slotkin, T. A. (2003) Fetal chlorpyrifos exposure: adverse effects on brain cell development and cholinergic biomarkers emerge postnatally and continue into adolescence and adulthood. *Environ. Health Perspect. 111*, 536−544.

(11) Perez-Fernandez, C., Morales-Navas, M., Guardia-Escote, L., Garrido-Cárdenas, J. A., Colomina, M. T., Giménez, E., and Sánchez-Santed, F. (2020) Long-term effects of low doses of Chlorpyrifos exposure at the preweaning developmental stage: A locomotor, pharmacological, brain gene expression and gut microbiome analysis. *Food Chem. Toxicol. 135*, 110865.

(12) Guardia-Escote, L., Basaure, P., Biosca-Brull, J., Cabré, M., Blanco, J., Pérez-Fernández, C., Sánchez-Santed, F., Domingo, J. L.,

and Colomina, M. T. (2020) APOE genotype and postnatal chlorpyrifos exposure modulate gut microbiota and cerebral short-chain fatty acids in preweaning mice. *Food Chem. Toxicol. 135*, 110872.
(13) Perez-Fernandez, C., Morales-Navas, M., Guardia-Escote, L., Colomina, M. T., Giménez, E., and Sánchez-Santed, F. (2020) Postnatal exposure to low doses of Chlorpyrifos induces long-term effects on 5C-SRTT learning and performance, cholinergic and GABAergic systems and BDNF expression. *Exp. Neurol. 330*, 113356.
(14) Perez-Fernandez, C., Morales-Navas, M., Aguilera-Sáez, L. M., Abreu, A. C., Guardia-Escote, L., Fernández, I., Garrido-Cárdenas, J. A., Colomina, M. T., Giménez, E., and Sánchez-Santed, F. (2020) Medium and long-term effects of low doses of Chlorpyrifos during the postnatal, preweaning developmental stage on sociability, dominance, gut microbiota and plasma metabolites. *Environ. Res. 184*, 109341.
(15) Lan, A., Kalimian, M., Amram, B., and Kofman, O. (2017) Prenatal chlorpyrifos leads to autism-like deficits in C57Bl6/J mice. *Environ. Health 16*, 43−43.
(16) Venerosi, A., Ricceri, L., Scattoni, M. L., and Calamandrei, G. (2009) Prenatal chlorpyrifos exposure alters motor behavior and ultrasonic vocalization in CD-1 mouse pups. *Environ. Health 8*, 12.
(17) Morales-Navas, M., Castaño-Castaño, S., Pérez-Fernández, C., Sánchez-Gil, A., Teresa Colomina, M., Leinekugel, X., and Sánchez-Santed, F. (2020) Similarities between the Effects of Prenatal Chlorpyrifos and Valproic Acid on Ultrasonic Vocalization in Infant Wistar Rats. *Int. J. Environ. Res. 17*, 6376.
(18) Ellenbroek, B., and Youn, J. (2016) Rodent models in neuroscience research: is it a rat race? *Dis. Models & Mech. 9*, 1079−1087.
(19) Collino, S., Martin, F.-P. J., and Rezzi, S. (2013) Clinical metabolomics paves the way towards future healthcare strategies. *Br. J. Clin. Pharmacol. 75*, 619−629.
(20) Dubois, B., Hampel, H., Feldman, H. H., Scheltens, P., Aisen, P., Andrieu, S., Bakardjian, H., Benali, H., Bertram, L., Blennow, K., Broich, K., Cavedo, E., Crutch, S., Dartigues, J.-F., Duyckaerts, C., Epelbaum, S., Frisoni, G. B., Gauthier, S., Genthon, R., Gouw, A. A., Habert, M.-O., Holtzman, D. M., Kivipelto, M., Lista, S., Molinuevo, J.-L., O'Bryant, S. E., Rabinovici, G. D., Rowe, C., Salloway, S., Schneider, L. S., Sperling, R., Teichmann, M., Carrillo, M. C., Cummings, J., and Jack, C. R., Jr. (2016) Preclinical Alzheimer's disease: Definition, natural history, and diagnostic criteria. *Alzheimer's Dementia 12*, 292−323.
(21) Cheung, P. K., Ma, M. H., Tse, H. F., Yeung, K. F., Tsang, H. F., Chu, M. K. M., Kan, C. M., Cho, W. C. S., Ng, L. B. W., Chan, L. W. C., and Wong, S. C. C. (2019) The applications of metabolomics in the molecular diagnostics of cancer. *Expert Rev. Mol. Diagn. 19*, 785−793.
(22) Song, Z., Wang, H., Yin, X., Deng, P., and Jiang, W. (2019) Application of NMR metabolomics to search for human disease biomarkers in blood. *Clin. Chem. Lab. Med. 57*, 417.
(23) Rinehart, N. J., Tonge, B. J., Iansek, R., McGinley, J., Brereton, A. V., Enticott, P. G., and Bradshaw, J. L. (2006) Gait function in newly diagnosed children with autism: Cerebellar and basal ganglia related motor disorder. *Dev. Med. Child Neurol. 48*, 819−824.
(24) Golden, C. E., Buxbaum, J. D., and De Rubeis, S. (2018) Disrupted circuits in mouse models of autism spectrum disorder and intellectual disability. *Curr. Opin. Neurobiol. 48*, 106−112.
(25) Sharma, A., Gokulchandran, N., Sane, H., Nivins, S., Paranjape, A., and Badhe, P. (2018) The Baseline Pattern and Age-related Developmental Metabolic Changes in the Brain of Children with Autism as Measured on Positron Emission Tomography/Computed Tomography Scan. *World J. Nucl. Med. 17*, 94−101.
(26) Siniscalco, D., Schultz, S., Brigida, A. L., and Antonucci, N. (2018) Inflammation and Neuro-Immune Dysregulations in Autism Spectrum Disorders. *Pharmaceuticals 11*, 56.
(27) Baio, J., Wiggins, L., Christensen, D. L., Maenner, M. J, Daniels, J., Warren, Z., Kurzius-Spencer, M., Zahorodny, W., Robinson, C., Rosenberg, White, T., Durkin, M. S., Imm, P., Nikolaou, L., Yeargin-Allsopp, M., Lee, L.-C., Harrington, R., Lopez, M., Fitzgerald, R. T., Hewitt, A., Pettygrove, S., Constantino, J. N., Vehorn, A., Shenouda, J., Hall-Lande, J., Van, K., Naarden, Braun, and Dowling, N. F. (2018) Prevalence of Autism Spectrum Disorder Among Children Aged 8 Years — Autism and Developmental Disabilities Monitoring Network, 11 Sites, United States, 2014. *MMWR Surveill. Summ. 67*, 1−23.
(28) Rasalam, A. D., Hailey, H., Williams, J. H. G., Moore, S. J., Turnpenny, P. D., Lloyd, D. J., and Dean, J. C. S. (2005) Characteristics of fetal anticonvulsant syndrome associated autistic disorder. *Dev. Med. Child Neurol. 47*, 551−555.
(29) Lutz, N. W., Béraud, E., and Cozzone, P. J. (2014) Metabolomic analysis of rat brain by high resolution nuclear magnetic resonance spectroscopy of tissue extracts. *J. Vis. Exp.*, 51829−51829.
(30) Barnes, S., Benton, H. P., Casazza, K., Cooper, S. J., Cui, X., Du, X., Engler, J., Kabarowski, J. H., Li, S., Pathmasiri, W., Prasain, J. K., Renfrow, M. B., and Tiwari, H. K. (2016) Training in metabolomics research. II. Processing and statistical analysis of metabolomics data, metabolite identification, pathway analysis, applications of metabolomics and its future. *J. Mass Spectrom. 51*, 535−548.
(31) Bazinet, R. P., and Layé, S. (2014) Polyunsaturated fatty acids and their metabolites in brain function and disease. *Nat. Rev. Neurosci. 15*, 771−785.
(32) Kornhuber, M. E., Kornhuber, J., Retz, W., and Riederer, P. (1993) L-glutamate and L-aspartate concentrations in the developing and aging human putamen tissue. *J. Neural Transm. Gen. Sect. 93*, 145−150.
(33) Blüml, S., Wisnowski, J. L., Nelson, M. D., Jr., Paquette, L., Gilles, F. H., Kinney, H. C., and Panigrahy, A. (2013) Metabolic Maturation of the Human Brain From Birth Through Adolescence: Insights From *In Vivo* Magnetic Resonance Spectroscopy. *Cerebral Cortex. 23*, 2944−2955.
(34) Kreis, R., Hofmann, L., Kuhlmann, B., Boesch, C., Bossi, E., and Hüppi, P. S. (2002) Brain metabolite composition during early human brain development as measured by quantitative in vivo ^{1}H magnetic resonance spectroscopy. *Magn. Reson. Med. 48*, 949−958.
(35) Li, Y., Shen, M., Stockton, M. E., and Zhao, X. (2019) Hippocampal deficits in neurodevelopmental disorders. *Neurobiol. Learn. Mem. 165*, 106945.
(36) Sohal, V. S., and Rubenstein, J. L. R. (2019) Excitation-inhibition balance as a framework for investigating mechanisms in neuropsychiatric disorders. *Mol. Psychiatry 24*, 1248−1257.
(37) Heyer, D. B., and Meredith, R. M. (2017) Environmental toxicology: Sensitive periods of development and neurodevelopmental disorders. *NeuroToxicology 58*, 23−41.
(38) Spear, L. P. (2000) The adolescent brain and age-related behavioral manifestations. *Neurosci Biobehav Rev . 24*, 417−463.
(39) Tremblay, M. W., and Jiang, Y.-H. (2019) DNA Methylation and Susceptibility to Autism Spectrum Disorder. *Annu. Rev. Med. 70*, 151−166.
(40) Ford, T. C., and Crewther, D. P. (2016) A Comprehensive Review of the (1)H-MRS Metabolite Spectrum in Autism Spectrum Disorder. *Front. Mol. Neurosci. 9*, 14−14.
(41) Pizzarelli, R., and Cherubini, E. (2011) Alterations of GABAergic signaling in autism spectrum disorders. *Neural Plast. 2011*, 297153−297153.
(42) Cellot, G., and Cherubini, E. (2014) GABAergic signaling as therapeutic target for autism spectrum disorders. *Front. Pediatr. 2*, 70−70.
(43) Ford, T. C., Nibbs, R., and Crewther, D. P. (2017) Increased glutamate/GABA+ ratio in a shared autistic and schizotypal trait phenotype termed Social Disorganisation. *NeuroImage Clin. 16*, 125−131.
(44) Shinohe, A., Hashimoto, K., Nakamura, K., Tsujii, M., Iwata, Y., Tsuchiya, K. J., Sekine, Y., Suda, S., Suzuki, K., Sugihara, G.-i., Matsuzaki, H., Minabe, Y., Sugiyama, T., Kawai, M., Iyo, M., Takei, N., and Mori, N. (2006) Increased serum levels of glutamate in adult patients with autism. *Prog. Neuro-Psychopharmacol. Biol. Psychiatry 30*, 1472−1477.

https://doi.org/10.1021/acschembio.1c00053
ACS Chem. Biol. 2021, 16, 753−765

(45) Shimmura, C., Suda, S., Tsuchiya, K. J., Hashimoto, K., Ohno, K., Matsuzaki, H., Iwata, K., Matsumoto, K., Wakuda, T., Kameno, Y., Suzuki, K., Tsujii, M., Nakamura, K., Takei, N., and Mori, N. (2011) Alteration of Plasma Glutamate and Glutamine Levels in Children with High-Functioning Autism. *PLoS One 6*, No. e25340.
(46) Rojas, D. C., Becker, K. M., and Wilson, L. B. (2015) Magnetic Resonance Spectroscopy Studies of Glutamate and GABA in Autism: Implications for Excitation-Inhibition Imbalance Theory. *Curr. Dev. Disord. Rep. 2*, 46−57.
(47) Rojas, D. C., Singel, D., Steinmetz, S., Hepburn, S., and Brown, M. S. (2014) Decreased left perisylvian GABA concentration in children with autism and unaffected siblings. *NeuroImage 86*, 28−34.
(48) Usui, N., Iwata, K., Miyachi, T., Takagai, S., Wakusawa, K., Nara, T., Tsuchiya, K. J., Matsumoto, K., Kurita, D., Kameno, Y., Wakuda, T., Takebayashi, K., Iwata, Y., Fujioka, T., Hirai, T., Toyoshima, M., Ohnishi, T., Toyota, T., Maekawa, M., Yoshikawa, T., Maekawa, M., Nakamura, K., Tsujii, M., Sugiyama, T., Mori, N., and Matsuzaki, H. (2020) VLDL-specific increases of fatty acids in autism spectrum disorder correlate with social interaction. *EBioMedicine. 58*, 102917.
(49) Mazahery, H., Stonehouse, W., Delshad, M., Kruger, M. C., Conlon, C. A., Beck, K. L., and von Hurst, P. R. (2017) Relationship between Long Chain n-3 Polyunsaturated Fatty Acids and Autism Spectrum Disorder: Systematic Review and Meta-Analysis of Case-Control and Randomised Controlled Trials. *Nutrients 9*, 155.
(50) El-Ansary, A. K, Ben Bacha, A. G, and Al- Ayahdi, L. Y (2011) Plasma fatty acids as diagnostic markers in autistic patients from Saudi Arabia. *Lipids Health Dis. 10*, 62.
(51) Orozco, J. S., Hertz-Picciotto, I., Abbeduto, L., and Slupsky, C. M. (2019) Metabolomics analysis of children with autism, idiopathic-developmental delays, and Down syndrome. *Transl. Psychiatry 9*, 243.
(52) Smith, A. M., King, J. J., West, P. R., Ludwig, M. A., Donley, E. L. R., Burrier, R. E., and Amaral, D. G. (2019) Amino Acid Dysregulation Metabotypes: Potential Biomarkers for Diagnosis and Individualized Treatment for Subtypes of Autism Spectrum Disorder. *Biol. Psychiatry 85*, 345−354.
(53) Zheng, H.-F., Wang, W.-Q., Li, X.-M., Rauw, G., and Baker, G. B. (2017) Body fluid levels of neuroactive amino acids in autism spectrum disorders: a review of the literature. *Amino Acids 49*, 57−65.
(54) Aldred, S., Moore, K. M., Fitzgerald, M., and Waring, R. H. (2003) Plasma Amino Acid Levels in Children with Autism and Their Families. *J. Autism. Dev. Disord. 33*, 93−97.
(55) Tărlungeanu, D. C., Deliu, E., Dotter, C. P., Kara, M., Janiesch, P. C., Scalise, M., Galluccio, M., Tesulov, M., Morelli, E., Sonmez, F. M., Bilguvar, K., Ohgaki, R., Kanai, Y., Johansen, A., Esharif, S., Ben-Omran, T., Topcu, M., Schlessinger, A., Indiveri, C., Duncan, K. E., Caglayan, A. O., Gunel, M., Gleeson, J. G., and Novarino, G. (2016) Impaired Amino Acid Transport at the Blood Brain Barrier Is a Cause of Autism Spectrum Disorder. *Cell 167*, 1481−1494 e1418..
(56) Wu, G., Fang, Y.-Z., Yang, S., Lupton, J. R., and Turner, N. D. (2004) Glutathione Metabolism and Its Implications for Health. *J. Nutr. 134*, 489−492.
(57) Kim, K. C., Kim, P., Go, H. S., Choi, C. S., Yang, S. I., Cheong, J. H., Shin, C. Y., and Ko, K. H. (2011) The critical period of valproate exposure to induce autistic symptoms in Sprague-Dawley rats. *Toxicol. Lett. 201*, 137−142.
(58) Alpay Savasan, Z., Yilmaz, A., Ugur, Z., Aydas, B., Bahado-Singh, R. O., and Graham, S. F. (2019) Metabolomic Profiling of Cerebral Palsy Brain Tissue Reveals Novel Central Biomarkers and Biochemical Pathways Associated with the Disease: A Pilot Study. *Metabolites 9*, 27.
(59) Pears, M. R., Cooper, J. D., Mitchison, H. M., Mortishire-Smith, R. J., Pearce, D. A., and Griffin, J. L. (2005) High Resolution ^{1}H NMR-based Metabolomics Indicates a Neurotransmitter Cycling Deficit in Cerebral Tissue from a Mouse Model of Batten Disease. *J. Biol. Chem. 280*, 42508−42514.

https://doi.org/10.1021/acschembio.1c00053
ACS Chem. Biol. 2021, 16, 753−765